13. D. M. Bushnell, J. N. Hefner, and R. L. Ash, "Effect of compliant wall motion on turbulent boundary layers," Phys. Fluids, 20, Pt. 2 (1977).
14. J. M. MacMichael, F. S. Klebanov, and N. E. Meese, "Experimental investigation of deformable surface drag," Viscous Friction Reduction [Russian translation], Mashinostroenie, Moscow (1984).
15. L. Prandtl, Essentials of Fluid Dynamics, Blackie, London (1952).
16. F. H. Clauser, "Turbulent boundary layers in adverse pressure gradients," J. Aero. Sci., 21, No. 2 (1954).
17. D. Hudson, Statistics for Physicists [Russian translation], Mir, Moscow (1967).
18. H. Schlichting, Boundary Layer Theory, 6th ed., McGraw-Hill, New York (1968).
19. R. Takaki and L. S. G. Kovasznay, "Statistical theory of vortex merger in the two-dimensional mixing layer," Phys. Fluids, 21, No. 2 (1978).
20. I. S. Berezin and N. P. Zhidkov, Calculation Methods [in Russian], Vol. 2, Fiz.-Mat. Lit., Moscow (1962).
21. K. N. Rao, R. Narasimha, and M. A. B. Narayanan, "The "bursting" phenomenon in a turbulent boundary layer," J. Fluid Mech., 48, No. 2 (1971).
22. P. R. Bandyopadhyay, "Period between bursting in turbulent boundary layers," Phys. Fluids, 25, No. 10 (1982).
23. M. J. Walsh and A. M. Lindemann, Optimization and Application of Riblets for Turbulent Drag Reduction, AIAA Paper No. 0347, New York (1984).
24. G. A. Kuz'min, O. A. Likhachev, and A. Z. Patashinskii, "Structures and their evolution in a turbulent shear layer," Prikl. Mekh. Tekh. Fiz., No. 5 (1983).

TURBULENT BOUNDARY LAYER ON THE ROTATING END OF A SWIRL CHAMBER

É. P. Volchkov, S. V. Semenov, and V. I. Terekhov

UDC 532.59.001.572

Aerodynamics and heat transfer in the neighborhood of a rotating disk have been studied by many investigators. A survey of such works can be found in [1], for example. Most of these studies examined the cases of rotation of a disk located in a free volume or exposed to an axial flow [1-3], as well as the interaction of a twisted flow with a stationary surface (a bibliography on this subject can be found in [4]).

Information on the interaction of a rotating disk with a twisted flow is limited to [5, 6]. The authors of [5] theoretically examined the turbulent boundary layer formed on a disk rotating at an angular velocity Ω and interacting with a gas flow which was itself rotating as a solid. A theoretical and experimental study was made in [6] of the laminar boundary layer on the rotating end wall of a swirl chamber. The angular velocity of the end was fixed, while the gas rotated in accordance with the law governing a free vortex.

In actual swirl chambers with an outlet containing a diaphragm, the rotation of the gas takes place in accordance with a complex law. As a first approximation, the flow outside the outlet hole is assumed to be a potential flow in which the circulation $\Gamma = v_0 r = \text{const}$, where v_0 is the circumferential component of velocity in the flow core. As was shown in [4, 7], such a law of flow rotation is observed with a change in the radius from the lateral wall of the chamber R to r* (r* determines the radius value where all of the gas enters into boundary layers on the end plates and travels through them into the region of the outlet hole). The rotation of a gas in a swirl chamber or tube not provided with a diaphragm occurs in accordance with the law of quasi-solid rotation at an angular velocity $\omega = v_0/r = \text{const}$.

Rotating end plates can be used in a number of vortex-type processing units to improve their efficiency. In these cases, the circumferential velocity of the flow decreases with approach toward the end wall. The velocity decreases not to zero, but to the linear velocity of rotation of the end at the given point. This alleviates the imbalance of centrifugal forces in the end boundary layer and preserves the radial pressure gradient in it, which leads

Novosibirsk. Translated from Zhurnal Prikladnoi Mekhaniki i Tekhknicheskoi Fiziki, No. 5, pp. 74-80, September-October, 1988. Original article submitted May 21, 1987.

 0021-8944/88/2905-0668$12.50

to a reduction in the end radial flow and displacement of the value of r^* toward the axis of the chamber.

1. Integral Momentum Relation for an End Boundary Layer. Friction Law. Here, within the framework of boundary-layer theory, we will examine a turbulent boundary layer on the flat rotating end of a swirl chamber. The gas above the surface rotates according to the law

$$v_0 = v_c(r/R)^{-m} \tag{1.1}$$

(v_c is the circumferential velocity at the side wall of the chamber). We have quasi-solid rotation of the gas at m = −1, while at m = 1 the situation corresponds to a potential law of rotation. The presence of the cylindrical side wall undoubtedly has an effect on the aerodynamics of the end layer and the chamber as a whole. However, it is assumed that this occurs in a narrow region near the wall, and this zone is not examined here.

In the study of turbulent rotating boundary layers in swirl chambers with a stationary end, the profile of circumferential velocity is described by the exponential relation $v_1/v_0 = (z/\delta_1)^n$, n = 1/7. It has been suggested [1, 2] that the profile near a disk rotating in a stationary volume be described by the relation $v_2/\Omega r = 1 - (z/\delta_2)^n$. Here, δ_1 and δ_2 are the thicknesses of the corresponding boundary layers. Assuming that the boundary layer formed with the joint rotation of the flow and disk has a thickness δ identical with δ_1 and δ_2, we find the profile of circumferential velocity in the form

$$v = v_1 + v_2 = v_0\xi^n + \Omega r(1 - \xi^n) \ (\xi = z/\delta). \tag{1.2}$$

Introducing the dimensionless circumferential velocity in the coordinate system connected with the disk $\bar{v} = (v - \Omega r)/(v_0 - \Omega r)$, in accordance with (1.2) we obtain

$$\bar{v} = \xi^n. \tag{1.3}$$

To approximate the radial component of velocity, we will use the approach proposed in [7]. The boundary layer is subdivided into two zones – the wall part $0 < z < \delta_m$, governed by the laws which govern boundary turbulence; the jet zone $\delta_m < z < \delta$, where jet mixing processes predominate (δ_m (Fig. 1a) corresponds to the maximum of radial velocity in the boundary layer). The profiles of radial velocity in these zones can be respectively described by an exponential relation and the Schlichting formula

$$\begin{gathered} \bar{u} = u/u_m = (z/\delta_m)^n \text{ for } 0 < z < \delta_m, \\ (u - u_0)/(u_m - u_0) = [1 - (z_1/b_1)^{3/2}]^2 \text{ for } \delta_m < z < \delta, \end{gathered} \tag{1.4}$$

where u_0 is the radial velocity in the flow core; u_m is the maximum value of radial velocity; $z_1 = z - \delta_m$; $b_1 = \delta - \delta_m$.

Figure 1a schematically depicts diagrams of the circumferential and radial components of gas velocity in the end boundary layer in the case where a forced vortex exists above the layer. Here, we introduce the parameter of the end twist $S = \Omega R/v_c$, characterizing the ratio of the linear circumferential velocity of the end to the circumferential velocity of the flow at the side wall of the chamber. In Fig. 1a, $S = \Omega/\omega > 1$, and the end radial flow is directed toward the periphery of the chamber. It is evident that the radial velocity in the boundary layer changes direction at S < 1.

Figure 1b illustrates the flow pattern on an end rotating in a swirl chamber with a diaphragm. However, this is not the only flow scheme possible. One of three patterns will be formed (Fig. 2), depending on the speed of rotation of the end in the boundary layer: 1) at $0 < S \leq 1$, the circumferential velocity of the end Ωr is less than the circumferential velocity of the flow v_0 over the entire radius of the chamber, and the radial gas flow in the boundary layer is directed toward the chamber axis; 2) with an increase in S from 1 to $\bar{r}_1^{-2}$, determined from the condition of equality of the circumferential velocities of the end and the gas flow at the border of the outlet hole $\Omega r_1 = v_c(R/r_1)$, the boundary layer has two regions separated by the value of the radius r_s (Fig. 1b). At $r > r_s$, the gas located near the end acquires a circumferential velocity greater than the velocity in the flow core and is thrown to the periphery of the chamber. Conversely, in the internal region ($r < r_s$), the rotation of the gas in the boundary layer is slowed and it moves toward the chamber axis; 3) more developed twisting of the end ($S > \bar{r}_1^{-2}$) leads to a situation whereby the end wall rotates faster than the gas, and the latter will be thrown toward the end walls of the chamber over its entire surface.

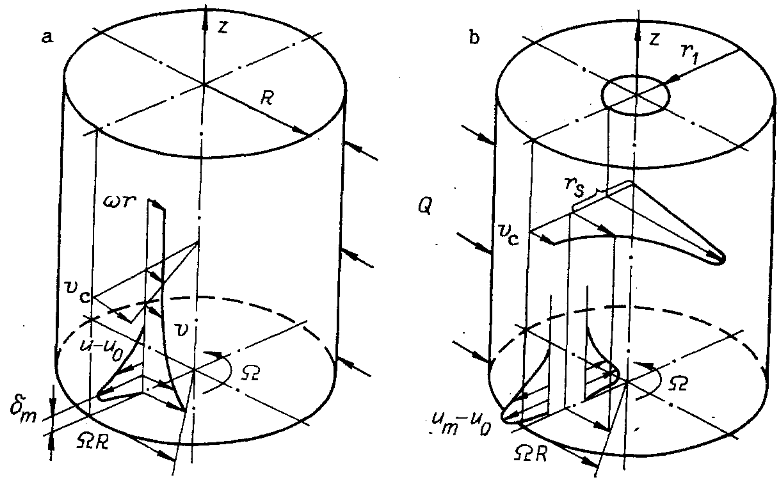

Fig.1

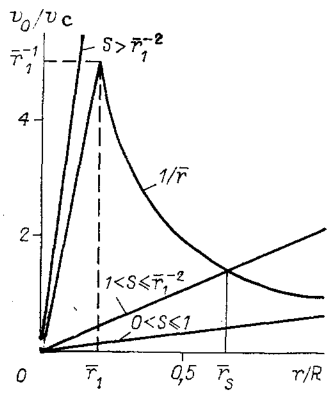

Fig. 2

We will write the equations of motion and continuity for the end boundary layer in a cylindrical coordinate system [1]:

$$u\frac{\partial u}{\partial r}+w\frac{\partial u}{\partial z}-\frac{v^2}{r}=-\frac{1}{\rho}\frac{\partial p}{\partial r}+\frac{1}{\rho}\frac{\partial \tau_{rz}}{\partial z}; \tag{1.5}$$

$$u\frac{\partial v}{\partial r}+w\frac{\partial v}{\partial z}+\frac{uv}{r}=\frac{1}{\rho}\frac{\partial \tau_{\varphi z}}{\partial z}; \tag{1.6}$$

$$\partial p/\partial z=0,\ \partial u/\partial r+u/r+\partial w/\partial z=0. \tag{1.7}$$

Here, τ_{rz}, and $\tau_{\varphi z}$ are components of the tensor of the shear stresses, equal to the sum of the viscous and turbulent components; u, v, and w are the radial, tangential, and axial components of velocity. Integrating (1.6) over the thickness of the end boundary layer with the use of continuity equation (1.7), after some simple transformations we obtain an integral equation to describe the conservation of angular momentum

$$\frac{d\,\mathrm{Re}_\varphi^{**}}{d\bar r}+\mathrm{Re}_\varphi^{**}\left\{\frac{1}{\bar r}-\frac{2\Omega R}{v_0-\Omega\bar r R}-\overline{W}\left[\frac{1}{\bar r}+\frac{1}{v_0-\Omega\bar r R}\times\right.\right.$$
$$\left.\left.\times\frac{\partial\left(v_0-\Omega\bar r R\right)}{\partial\bar r}+\frac{2\Omega R}{v_0-\Omega\bar r R}\right]\right\}=\frac{(\tau_{\varphi z})_w}{\rho\left(v_0-\Omega\bar r R\right)u_m}\frac{u_m R}{\nu}. \tag{1.8}$$

Integration was done with the boundary conditions

$$z=0:\ u=w=0,\ v=\Omega r,\ \tau_{\varphi z}=(\tau_{\varphi z})_w,$$

$$z=\delta:\ u=u_0=0,\ w=0,\ v=v_0,\ \tau_{\varphi z}=0.$$

Here, we examined the case when the radial component of velocity in the core of the flow u_0 might be less than the circumferential velocity: $u_0 \ll v_0$. In Eq. (1.8), we introduced the following notation: $\delta_\varphi^{**} = \int_0^\delta \bar{u}(1-\bar{v})\,dz$ is the momentum thickness; $\mathrm{Re}_\varphi^{**} = u_m\delta^{**}/\nu$; $\overline{W} = \int_0^\delta \bar{u}\bar{v}dz/\delta_\varphi^{**}$; $\bar{r} = r/R$ is the dimensionless radius. Taking (1.1) for the law of change in the circumferential component of velocity outside the boundary layer and introducing the parameter S, we rewrite Eq. (1.8):

$$\frac{d\,\mathrm{Re}_\varphi^{**}}{d\bar{r}} + \frac{\mathrm{Re}_\varphi^{**}}{\bar{r}}\left\{[1-\overline{W}(1-m)] - S\frac{2+\overline{W}(1-m)}{\bar{r}^{-(m+1)}-S}\right\} = \frac{c_{f\varphi}}{2}\frac{u_m R}{\nu} \tag{1.9}$$

($c_{f\varphi}/2 = (\tau_{\varphi z})_w/[\rho u_m(v_0 - \Omega\bar{r}R)]$ is the friction coefficient in the circumferential direction).

To solve Eq. (1.9), we need to know the change in u_m over the radius of the end and the connection between the friction coefficient $c_{f\varphi}/2$ and the integral parameters of the boundary layer. To find these relations, we will use the method in [4, 7]. The latter provides good agreement with the experimental data for a stationary end.

To determine the dependence of u_m on the radius of the end, we write Eq. (1.5) with $z = \delta_m$, having set $(\partial\tau_{rz}/\partial z)_{z=\delta_m} \to 0$ in a first approximation:

$$u_m\frac{\partial u_m}{\partial\bar{r}} - \frac{v_m^2}{\bar{r}} = -\frac{1}{\rho}\frac{\partial p}{\partial\bar{r}}. \tag{1.10}$$

Here, v_m is the value of circumferential velocity determined from Eqs. (1.1) and (1.2) for $z = \delta_m$:

$$v_m = v_c\bar{r}^{-m}\xi_m^n + \Omega\bar{r}R(1-\xi_m^n). \tag{1.11}$$

Assuming that $v_0^2/r \gg u_0\partial u_0/\partial r$ in severely swirled flows and assuming that the flow is for the most part inviscid with a profile of circumferential velocity which is constant along z, we use (1.6) to write the following for $z > \delta$

$$u_0\frac{\partial u_0}{\partial\bar{r}} - \frac{v_0^2}{\bar{r}} \simeq -\frac{v_0^2}{\bar{r}} = -\frac{1}{\rho}\frac{\partial p}{\partial\bar{r}}. \tag{1.12}$$

Equating the left sides of Eqs. (1.10) and (1.12) and having inserted (1.1) and (1.11) into them, with allowance for $u_0 \ll v_c$ we obtain the following after integration

$$\left(\frac{u_m}{v_c}\right)^2 = -2\int\bar{r}^{-(2m+1)}\{1-\xi_m^{2n}[1+(\xi_m^{-n}-1)S\bar{r}^{(m+1)}]^2\}\,d\bar{r} + C_1. \tag{1.13}$$

We agree to consider motion of the radial component of velocity toward the chamber axis to be the positive direction. The constant of integration C_1 in (1.13) is determined below in an examination of specific cases of interaction of a flow and an end wall on the basis of the corresponding boundary conditions.

In accordance with [7], we take $\xi_m = \delta_m/\delta = 0.15$. The use of a constant value of ξ_m appreciably simplifies the calculations: it is no longer necessary to solve an integral relation for the radial direction. The numerical values of the coefficients used in integral relation (1.9) and later calculations, determined through ξ_m, are equal to [7]:

$$\bar{\delta}_\varphi^{**} = \delta_\varphi^{**}/\delta = 0.0941,\quad \overline{W} = 4.46,\quad \overline{C} = \int_0^\delta \bar{u}dz/\delta_\varphi^{**} = 5.462. \tag{1.14}$$

We will examine flow in the coordinate system connected with the rotating end. We will assume that the laws governing friction and the distribution of the shear-stress components in this system correspond to the case of interaction of a vortical flow with a stationary end. Then, using the conclusion reached in [7], we write the expression for the coefficient of friction in the circumferential direction

$$\frac{c_{f\varphi}}{2} = \frac{(\tau_{\varphi z})_w}{\rho u_m(v_0 - \Omega\bar{r}R)} = \frac{B}{2}\xi_m^{-3/28}(\mathrm{Re}_\varphi^{**})^{-1/4}\left(\frac{1+\mathrm{tg}^2\alpha}{\mathrm{tg}^2\alpha}\right)^{3/8}, \tag{1.15}$$

where $B/2 \approx 0.0128$. It is evident that the friction coefficient $c_{f\varphi}/2$ is connected with the parameter S through the angle of twist of the flow in the end boundary layer $\tan\alpha = f(\bar{r}, S)$. In accordance with (1.3) and (1.4), in the chosen coordinate system the angle of twist in the wall part ($0 < z < \delta_m$) is constant and is determined by the expression

$$\operatorname{tg}\alpha = u/(v - \Omega r) = \xi_m^{-1/7} u_m/(v_0 - \Omega \bar{r} R). \tag{1.16}$$

The ratio of the radial and circumferential components of the shear stresses is also determined by Eq. (1.16) and changes as follows for a law of change of circumferential velocity over the radius in the form (1.1):

$$\operatorname{tg}\alpha = (\tau_{rz})_w/(\tau_{\varphi z})_w = \frac{u_m}{v_c} \frac{\xi_m^{-1/7}}{\bar{r}^{-m} - S\bar{r}}. \tag{1.17}$$

Thus, the resulting expressions for u_m (1.13), $c_f/2$ (1.15), and tan α (1.17) make it possible to solve Eqs. (1.9) for any degree of twist of the end S and with an arbitrarily assigned law of gas rotation.

2. Solution of the Integral Relation for Quasi-Solid Rotation of the Flow. For a flow rotating in accordance with the law for a solid (m = −1), Eq. (1.9) has the form

$$\frac{d\mathrm{Re}_\varphi^{**}}{\partial \bar{r}} + \frac{\mathrm{Re}_\varphi^{**}}{\bar{r}}\left(\frac{1 - 2\overline{W} - 3S}{1 - S}\right) = -\frac{c_{f\varphi}}{2}\frac{u_m R}{\nu}. \tag{2.1}$$

We will restrict ourselves to examining a flow having an angular velocity which is less than the velocity of the disk (S > 1). A diagram of such a flow is shown in Fig. 1a. With the boundary condition $\bar{r} = 0$, $u_m = 0$, we find the following from (1.13)

$$u_m/v_c = -\bar{r}\{[S - \xi_m^{1/7}(S - 1)]^2 - 1\}^{0,5}. \tag{2.2}$$

Having inserted (2.2) into (1.7), we obtain the following for tan α

$$\operatorname{tg}\alpha = -\{[S - \xi_m^{1/7}(S - 1)]^2 - 1\}^{0,5}/[\xi_m^{1/7}(1 - S)]. \tag{2.3}$$

It is evident from (2.3) that in the case of rotation of the gas above a rotating disk in accordance with the solid law, tan α does not change over the radius. Having inserted the resulting expression into Eq. (1.15) for the friction coefficient $c_{f\varphi}/2$, with allowance for (2.2) we integrate Eq. (2.1) with the boundary condition $\bar{r} = 0$, $\mathrm{Re}_\varphi^{**} = 0$:

$$\mathrm{Re}_\varphi^{**} = \left(\frac{v_c R}{\nu}\right)^{0,8} \bar{r}^{1,6} A(S). \tag{2.4}$$

Here, $v_c = \omega R$; A(S) is a quantity which depends on the degree of twist S:

$$A(S) = \left\{\frac{1.25\frac{B}{2}\xi_m^{-3/28}[(1 + \operatorname{tg}^2\alpha)/\operatorname{tg}^2\alpha]^{3/8}\{[S - \xi_m^{1/7}(S - 1)]^2 - 1\}^{0,5}}{2 + 1.25(1 - 2\overline{W} - 3S)/(1 - S)}\right\}^{0,8}.$$

The value of Re_φ^{**}, together with the relation for the maximum of radial velocity u_m, makes it possible to determine all of the geometric and flow-rate parameters of the boundary layer. Thus, the volumetric rate of flow of the gas transported by the boundary layer in the radial direction can be found from the expression

$$Q_t = 2\pi r \int_0^\delta u\,dz = 2\pi \bar{r} \bar{C}\, \mathrm{Re}_\varphi^{**}\left(\frac{v_c R}{\nu}\right)^{-1} v_c R^2 \tag{2.5}$$

(the coefficient $\bar{C}$ was obtained in (1.14)). In [5], the rate of flow through the boundary layer Q_t was expressed by the dimensionless complex $q = Q_t(\Omega r^2/\nu)^{0.2}/\pi r^3 \Omega$. Reducing Eq. (2.5) to this form with the use of (2.4), we write $q = 2\bar{C}A(S)S^{-0.8}$.

In such notation, the rate of flow through the boundary layer is determined only by the degree of twist of the end S. Figure 3 shows estimates obtained as a function of S (curve 1). At S = 1, the gas and the disk rotate as one, and there is no boundary layer on the disk (q = 0). In the other limiting case (1/S → 0), we have rotation of the disk in a stationary volume and a maximum rate of flow through the boundary layer. Curve 2 shows the results calculated in [5]. It is evident that the solutions are in agreement.

3. Solution of the Integral Relation in the Interaction of a Rotating End with a Free Vortex (m = 1). Fundamentally different flow patterns may develop in the boundary layer, depending on the parameter S. First we will examine slight rotation of the end ($0 < S \leqslant 1$). The boundary layer begins to form near the side wall of the chamber. Thus, in integrating (1.13), we adopt the boundary condition $u_m = 0$ for $\bar{r} = 1$. Also assuming that $u_c \ll v_c$, as a result of integration we have

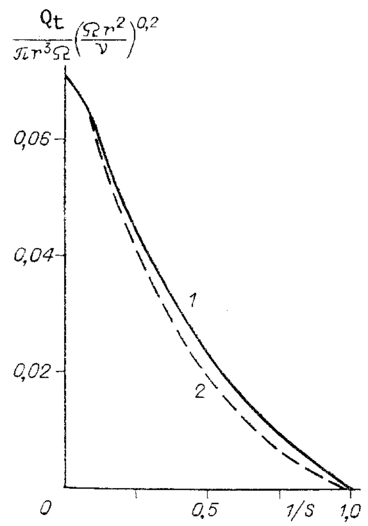

Fig. 3

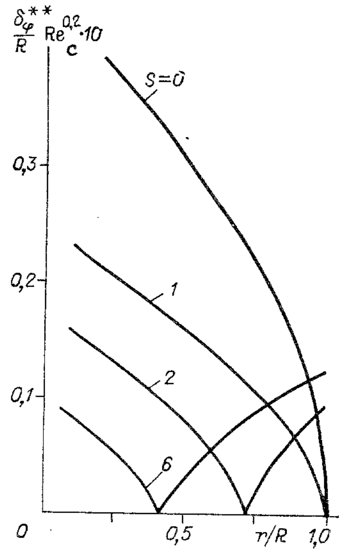

Fig. 4

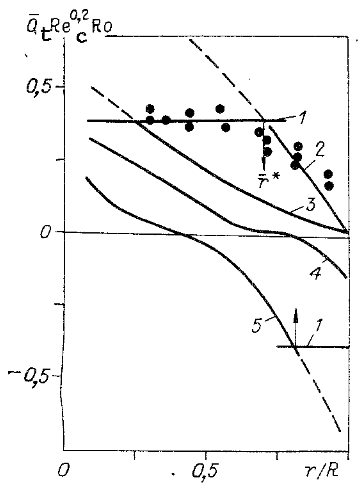

Fig. 5

$$u_m/v_c = \{(1-\xi)^{2/7}(\bar{r}^{-2}-1) + S[4\xi_m^{1/7}(1-\xi_m^{1/7})\ln\bar{r} - S(1-\xi_m^{1/7})^2(1-\bar{r}^2)]\}^{0.5}. \tag{3.1}$$

With values of the end rotation parameter within the range $1 < S \leq \bar{r}_1^{-2}$, formation of the boundary layer begins not near the side wall, but at the periphery of the radius $\bar{r}_s$. This is determined from the condition $\Omega r_s = v_0$ (Fig. 1b). The value of the radius $\bar{r}_s = S^{-0.5}$ found from the given equality is the boundary condition in the solution of the equation for the maximum of radial velocity (1.13) and the integral momentum relation, i.e., with $\bar{r} = S^{-0.5}$ $u_m = 0$, $\mathrm{Re}_\varphi^{**} = 0$. Gas begins to flow from the periphery of this radius in opposite directions, forming two boundary layers: at $\bar{r} < \bar{r}_s$, the gas moves toward the chamber axis; at $\bar{r} > \bar{r}_s$, the gas moves toward the side wall of the chamber. We find from (1.13) that

$$u_m/v_c = \pm\{|(1-\xi_m)^{2/7}(\bar{r}^{-2}-S) + S[4\xi_m^{1/7}(1-\xi_m^{1/7})\ln(\bar{r}S^{0.5}) - S(1-\xi_m^{1/7})^2(S^{-1}-\bar{r}^2)]|\}^{0.5}. \tag{3.2}$$

The sign in the right side of Eq. (3.2) is determined in accordance with the chosen positive direction of u_m: at $r < r_s$, u_m is positive; at $r > r_s$, it is negative. Inserting (3.1) and (3.2) into Eq. (1.17), we obtain the corresponding relations for tan α. This leaves one unknown, Re_φ^{**}, in integral relation (1.9):

$$\frac{d\mathrm{Re}_\varphi^{**}}{d\bar{r}} + \frac{\mathrm{Re}_\varphi^{**}}{\bar{r}}\left(\frac{1-3S\bar{r}^2}{1-S\bar{r}^2}\right) = -\frac{B}{2}\,\xi_m^{-3/28}(\mathrm{Re}_\varphi^{**})^{-1/4}\left(\frac{1+\mathrm{tg}^2\,\alpha}{\mathrm{tg}^2\,\alpha}\right)^{3/8}\frac{u_m R}{\nu}. \tag{3.3}$$

The solution of Eq. (3.3) by the Runge–Kutta method on a computer gave us the characteristics of the boundary layer: the momentum thickness δ_φ^{**}, the flow rate Q_t, the friction coefficient, etc.

Figure 4 shows the change in the dimensionless momentum thickness over the radius of the end $\bar{r}$ for different values of the end twist parameter S. It is evident that twisting of the end reduces the thickness of the boundary layer. For S > 1, the boundary layer begins to grow in both directions from the periphery of the corresponding radius r_s. Meanwhile, the thicknesses of these boundary layers are of the same order of magnitude.

Figure 5 shows the change in the complex $\bar{Q}_t Ro\ Re_c^{0.2}$ over the radius of the chamber. Here, $\bar{Q}_t = Q_t/Q$ is the relative rate of flow of the gas through the end boundary layer; $Ro = Q/v_c R^2$ is the Rossby number, characterizing the intensity of swirling of the gas at the chamber inlet; $Re_c = v_c R/\nu$ is the Reynolds number at the inlet. Straight line 1 characterizes the case when all of the gas entering the chamber is concentrated in the boundary layers, i.e., $\bar{Q}_t = 0.5Q$. The calculations were performed for $Re_c = 1.4 \cdot 10^5$ and Ro = 0.085. Curve 2 is the result of calculation of the rate of flow through the end boundary layer for a stationary end (S = 0). Lines 1 and 2 intersect at $\bar{r} = \bar{r}^* \simeq 0.7$. The experimental points shown from [7] also correspond to flow in a chamber with a stationary end. It can be seen that these results agree with the calculated results as well. Line 3 shows results calculated for S = 1. In this case, the intersection with line 1 occurs at $r^* = 0.25$. Thus, through flow occurs over most of the chamber volume within a wide range of values. The boundary layer in the case S = 1 transports roughly half as much fluid and becomes half as thick (Fig. 4) as in the case of a stationary end.

Let us analyze the results of calculations for the range of values of the end rotation parameter $1 < S \leq \bar{r}_1^{-2}$, which are shown in Fig. 5 by curves 4 and 5 for S = 2 and 6, respectively. It is evident that in the region $\bar{r} < r_s$, flow rate through the boundary layer toward the chamber axis decreases with an increase in S. In the region $\bar{r} > r_s$, the fraction of gas thrown toward the side wall increases. The thickness of the boundary layer behaves in a similar manner (increasing for S = 2 and 6, Fig. 4). The gas driven toward the periphery of the end should undoubtedly return to the main flow in the chamber. This will in turn lead to an increase in radial velocity u_0. Gas begins to be recirculated between the main flow and the boundary layer, with the fraction of recirculated gas increasing as S increases.

LITERATURE CITED

1. L. A. Dorfman, Hydrodynamic Resistance and Heat Transfer of Rotating Bodies, Fizmatgiz, Moscow (1960).
2. E. Truckenbrodt, "Die turbulente Strömung an einer angeblasenen rotierenden Scheibe," Z. Angew. Math. Mech., 34, 150 (1954).
3. T. Cebeci and D. E. Abbot, "Boundary layers on a rotating disk," AIAA J., 13, No. 6 (1975).
4. É. P. Volchkov, S. V. Semenov, and V. I. Terekhov, "End boundary layer in a swirl chamber," in: Structure of Forced and Thermogravitational Flows [in Russian], Novosibirsk (1983).
5. B. G. Newman, "Flow and heat transfer on a disk rotating beneath a forced vortex," AIAA J., 21, No. 8 (1983).
6. W. J. Shakespeare and E. K. Levy, "Laminar boundary layer near the rotating end wall of a confined vortex," J. Fluids Eng., No. 2 (1982).
7. É. P. Volchkov, S. V. Semenov, and V. I. Terekhov, "Aerodynamics of the end boundary layer in a swirl chamber," Zh. Prikl. Mekh. Tekh. Fiz., No. 5 (1986).